Cerebral Cortex June 2012;22:1318–1332
doi:10.1093/cercor/bhr212
Advance Access publication August 1, 2011

Associative Properties of the Perirhinal Network

Gunes Unal, John Apergis-Schoute and Denis Paré

Center for Molecular and Behavioral Neuroscience, Rutgers, The State University of New Jersey, Newark, NJ 07102, USA

Unal and Apergis-Schoute have contributed equally to this work

Address correspondence to Denis Paré, Center for Molecular and Behavioral Neuroscience, Rutgers, The State University of New Jersey, 197 University Avenue, Newark, NJ 07102, USA. Email: pare@andromeda.rutgers.edu.

The perirhinal area is a rostrocaudally oriented cortical region involved in recognition and associative memory. It receives topographically organized transverse projections from high-order neocortical areas and is endowed with intrinsic longitudinal connections that distribute neocortical inputs rostrocaudally. Earlier work has revealed that neocortical inputs strongly recruit perirhinal interneurons located at the same transverse level, limiting the depolarization of principal cells. In contrast, at a distance, neocortical stimuli only evoke excitation because longitudinal perirhinal pathways do not engage interneurons. This raises the possibility that the perirhinal network allows for Hebbian-like associative interactions between coincident and spatially distributed inputs. To test this, we analyzed the effects of theta-frequency neocortical stimulation using simultaneous field potential recordings and optical imaging in the whole guinea pig brain in vitro. Theta-frequency stimulation (TFS) at one neocortical site resulted in a prolonged input-specific response depression at all perirhinal levels. In contrast, paired TFS of 2 distant neocortical sites resulted in a prolonged response potentiation to the paired inputs, suggesting that longitudinal perirhinal connections can support associative interactions between coincident but spatially distributed inputs. Moreover, we found that induction of these 2 forms of plasticity depended on the competing influence of glutamate group I metabotropic and NMDA receptors, respectively.

Keywords: inhibition, learning, memory, perirhinal, synaptic plasticity

Introduction

It is well established that the perirhinal cortex plays a pivotal role in memory. Indeed, perirhinal lesions cause recognition memory impairments (Zola-Morgan et al. 1989; Gaffan and Murray 1992; Meunier et al. 1993, 1996; Suzuki et al. 1993) that compare with, or are more severe than, those caused by hippocampal and entorhinal lesions (Aggleton et al. 1986; Murray and Mishkin 1986; Meunier et al. 1993; Leonard et al. 1995; Murray et al. 2005). Moreover, perirhinal lesions cause a severe associative memory deficit within and across sensory modalities (Murray et al. 1993; Higuchi and Miyashita 1996; Buckley and Gaffan 1998; Parker and Gaffan 1998; Goulet and Murray 2001), including auditory–somatosensory associations where perirhinal lesions were found to impair fear conditioning to discontinuous but not to continuous tones (Lindquist et al. 2004; Kholodar-Smith et al. 2008; Bang and Brown 2009a).

Consistent with this, the perirhinal cortex receives inputs from high-order associative cortical areas for each sensory modality. Most of these neocortical inputs originate from a strip of cortex that borders the perirhinal cortex laterally (Deacon et al. 1983; Room and Groenewegen 1986; Suzuki and Amaral 1994; Burwell and Amaral 1998a) and is termed "ventral temporal association cortex" in guinea pigs (Uva et al. 2004). Moreover, they are organized topographically (Fig. 1*A*) with rostral areas mainly targeting anterior perirhinal levels and posterior ones focusing on caudal parts of the perirhinal cortex. However, previous in vitro physiological studies have revealed that neocortical stimuli elicit neuronal responses that propagate to the entire rostrocaudal extent of the perirhinal cortex (Biella et al. 2001, 2010; Martina et al. 2001). Importantly, interruption of intrinsic neocortical versus perirhinal pathways with restricted knife cuts revealed that the propagation of neocortical activity did not occur in the neocortex but depended on longitudinal axonal pathways coursing in the perirhinal cortex itself and/or the external capsule (Martina et al. 2001). Consistent with this, small tracer injections in the neocortex (Deacon et al. 1983; Room and Groenewegen 1986) or perirhinal cortex (Witter et al. 1986; Lavenex et al. 2004) produce anterograde labeling throughout the rostrocaudal extent of the perirhinal cortex, indicating that the propagation of neocortical signals in the perirhinal cortex depends on neocortical and perirhinal neurons with longitudinal axons (see also Burwell and Amaral 1998b).

However, the effect of neocortical stimuli varies with the longitudinal distance between the neocortical stimulation site and the recorded perirhinal neuron (Biella et al. 2001; Martina et al. 2001). Neocortical stimulation sites located at the same rostrocaudal level as the recorded cells evoke large inhibitory post-synaptic potentials that curtail the initial excitatory post-synaptic potential. This observation is consistent with the findings of anterograde tracing studies where it was found that axons arising in the ventral temporal association cortex and ending in rostrocaudal register in the perirhinal cortex form asymmetric synapses with both principal neurons and local-circuit perirhinal cells (Pinto et al. 2006). In contrast, rostrocaudally distant sites evoke apparently pure excitatory responses, presumably because longitudinal perirhinal pathways do not engage feed-forward inhibitory interneurons (Biella et al. 2001; Martina et al. 2001). Although the latter conclusion awaits confirmation using anterograde tracing at the electron microscopic level, there are precedents in the literature for the differential recruitment of local-circuit cells by short- versus long-range cortico-cortical pathways. For instance, in the medial prefrontal cortex, Melchitzky et al. (1998) reported a 5-fold higher proportion of cortico-cortical synapses on local-circuit cells in short-range compared with long-range connections, a conclusion that was supported in a subsequent electrophysiological study (Gonzalez-Burgos et al. 2000).

The physiological findings reviewed above have important implications for associative perirhinal functions. First, they indicate that via longitudinal connections, distributed neocortical activation patterns can propagate longitudinally and converge on subsets of perirhinal cells (Fig. 1*A*). Second,

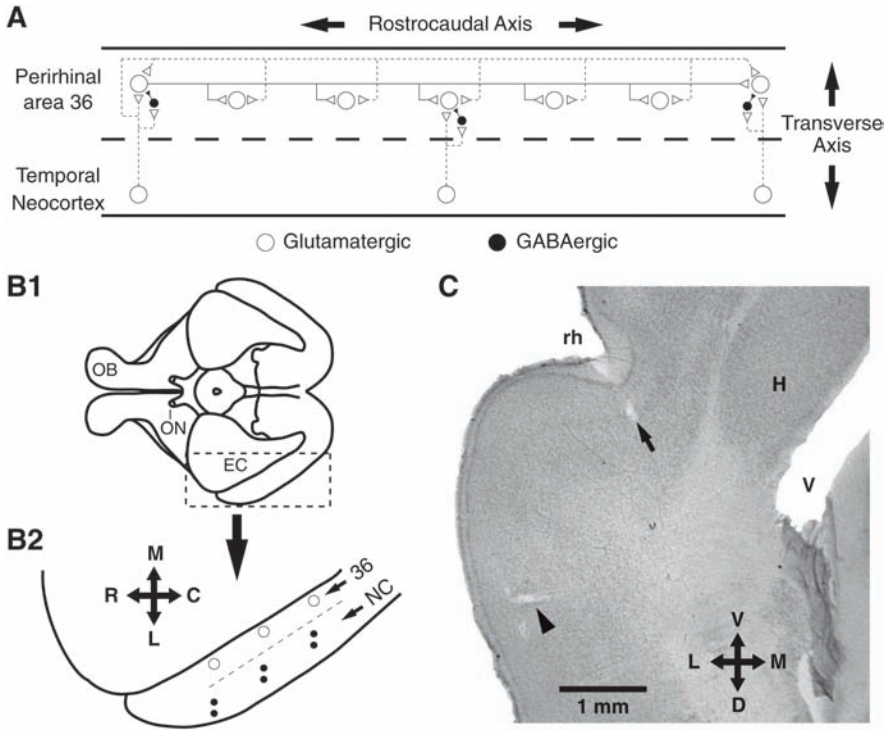

Figure 1. Experimental setup. (*A*) Organization of neocortical inputs and intrinsic perirhinal connections, as inferred from previous electrophysiological and tracing studies. Dashed lines indicate neocortical axons whereas continuous lines indicate perirhinal axons. Neocortical neurons contribute stronger projections to perirhinal levels in transverse register with them where they contact both glutamatergic principal cells and feed-forward inhibitory interneurons. Neocortical neurons and principal perirhinal neurons contribute axons that course longitudinally in the perirhinal cortex. Long-range neocortical and perirhinal longitudinal axons do not contact distant local circuit cells. (*B1*) Ventral view of guinea pig brain. Area delimited by dashed line is expanded below. (*B2*) Recording sites in perirhinal area 36 (empty circles) and stimulation sites in ventral temporal neocortex (pairs of black dots). (*C*) Coronal section showing electrolytic lesions performed at the end of an experiment to mark a neocortical stimulation site (arrowhead) and a recording site in perirhinal area 36 (arrow). Crosses indicate orientation (R, rostral; C, caudal; M, medial; L, lateral; D, dorsal; V, ventral). Other abbreviations: EC, entorhinal cortex; H, hippocampus; NC, neocortex; OB, olfactory bulb; ON, optic nerve; rh, rhinal sulcus; V, ventricle.

activation of a point source in the neocortex recruits perirhinal inhibitory interneurons at the corresponding transverse level (Fig. 1*A*), limiting the depolarization of principal cells. Third, because longitudinal axons within the perirhinal cortex do not engage feed-forward interneurons (Fig. 1*A*), simultaneous activation of 2 distant neocortical sites should shift the balance toward excitation in perirhinal cells receiving direct neocortical inputs. Given the well-established role of coincident neuronal activity in synaptic plasticity and evidence indicating that this mechanism is at play in the perirhinal cortex (Bilkey 1996; Ziakopoulos et al. 1999), this process might allow the perirhinal network to associate coincident but spatially distributed neocortical inputs. One might argue that there is nothing unique about the perirhinal cortex in this respect. After all, there are numerous well-documented examples in cortex where pairing of 2 inputs ending at different dendritic sites on the same pyramidal neuron undergo associative long-term potentiation (LTP). However, the perirhinal associative plasticity we are referring to is of a different nature. In the case of the perirhinal cortex, inputs from different sectors of the neocortex predominantly end at different rostrocaudal levels of the perirhinal cortex. As a result, associative interactions are not only dependent on within-cell mechanisms but also on long-range synaptic interactions supported by the intrinsic system of longitudinal connections that is so prominent in the perirhinal cortex. Thus, the present study was undertaken to examine how the perirhinal network might implement such associative interactions.

Materials and Methods

The Isolated and Arterially-Perfused Whole-Brain Preparation

Experiments were conducted on 96 Hartley guinea pigs (200–250 g, 3–5 weeks old) in accordance with the NIH Guide for the Care and Use of Laboratory Animals and with the approval of the Institutional Animal Care and Use committee of Rutgers University. Our approach to the preparation of the whole guinea pig brain kept in vitro is based on initial descriptions (de Curtis et al. 1991; Muhlethaler et al. 1993). Prior to the experiments, 2 cold (10 °C) solutions were prepared: a perfusate and a superfusate. Their composition was identical except for the addition of Dextran 70 (3%) to the perfusate. Otherwise, the 2 solutions contained (in mM) 126 NaCl, 2.5 KCl, 1.25 NaH_2PO_4, 1 $MgCl_2$, 2 $CaCl_2$, 26 $NaHCO_3$, and 10 glucose. Both solutions were saturated with an oxygenated gas mixture (95% O_2, 5% CO_2).

Animals were first deeply anesthetized with pentobarbital (60 mg/kg, intraperitoneal [i.p.]), ketamine (80 mg/kg, i.p.), and xylazine (12 mg/kg, i.p.) and then perfused transcardially with the cold, oxygenated perfusate. During the perfusion, an extensive craniotomy was performed and the dura mater was cut on the midline. At this point, the perfusion was interrupted, the cranial nerves and the carotid arteries sectioned, and the brain rapidly transferred to the recording chamber. The brain was positioned with its ventral surface up and a polyethylene cannula was inserted into the basilar artery. As the arterial perfusion was started, the leaking arteries were ligated. A peristaltic pump delivered the perfusate at a rate of 7 mL per minute. In addition, the brain was continuously superfused.

Once the leaking arteries were tied off, the temperature of the bath and recording chamber was increased to 29–31 °C at a rate of 0.2 °C per minute. A thermostat connected to a heat exchanger plate controlled the temperature of the perfusate and superfusate.

Stimulating and Recording Procedures

Electrophysiology

Stimulating and recording electrodes were positioned under visual control while the temperature of the brain was gradually increased. Although area 36 also receives substantial inputs from the insular and entorhinal cortices (Burwell and Amaral 1998b), the present study focused on inputs arising from the laterally adjacent ventral temporal association cortex. Based on earlier descriptions (Suzuki 1996), it appears that the ventral temporal association cortex corresponds to areas Te2 and Te3 of rats.

As shown in Figure 1*B*, 3 tungsten recording microelectrodes were positioned at different rostrocaudal levels of perirhinal area 36 at a depth of approximately 300 μm, corresponding to layer III (Fig. 1*B2*, empty circles). This depth was chosen because earlier field potential and current source density analyses have revealed that neocortical stimuli delivered in the temporoparietal region evoke maximal current sinks and field potential responses in layer III of area 36 (Biella et al. 2001, 2002). In addition, 3 pairs of stimulating electrodes (tip separation: 200 μm) were inserted at the same depth in the laterally adjacent neocortex (Fig. 1*B2*, dots), in rostrocaudal register with the recording area 36 electrodes. These stimulating electrodes were positioned 2 mm lateral to the recording electrodes, based on an earlier study that characterized the cytoarchitecture of this cortical region in guinea pigs (Uva et al. 2004). The signals picked up by the recording electrodes were observed on an oscilloscope, digitized at 20 kHz, and stored on a hard disk for off-line analysis with Igor (IGOR; WaveMetrics, Lake Oswego, OR).

Imaging

When the temperature of the brain reached 23 °C, the voltage-sensitive dye di-2-ANEPEQ (Invitrogen, Eugene, OR; 1.6 mg dissolved in 100 mL of perfusate) was applied to the brain via arterial perfusion for 14 min. The initial dye solution is then collected, filtered, and applied repetitively for a total duration of 90 min. This dye is taken up by neurons and rapidly signals changes in their membrane potential by changes in fluorescence intensity. This single dye application allowed recording of large optical signals for >2 h. The optical signal was observed through an epifluorescence microscope positioned above the perirhinal region (field of view: 10 by 7.6 mm) and collected with a CCD camera (MiCAM02, SciMedia, Costa Mesa, CA) at a frame rate of 200 Hz. Optical data is expressed as delta F/F. While our measurements focused on area 36, it is possible that some of the optical signals, especially those recorded most medially, originated in area 35. However, because area 35 is located within the rhinal fissure, its contribution to the neocortically elicited optical signals was most likely small.

Induction of Activity-Dependent Synaptic Plasticity

We attempted to induce activity-dependent plasticity only once in each brain. In the control phase, 10 electrical stimuli (300 μs, 0.5 mA; 0.1 Hz) were applied at each neocortical site and evoked responses averaged for each site separately. Then, in the induction phase, thirty 1-s trains of stimuli (8 Hz), each followed by a 0.5 s stimulus-free period, were applied at 1 or 2 neocortical sites. Hereafter, this stimulation protocol will be referred to as theta-frequency stimulation (TFS). To minimize bleaching of the dye, we did not attempt to obtain a continuous measure of changes in response amplitudes over time. Rather, beginning 5 and 30 min after TFS, single shocks were applied at each neocortical stimulation site 10 times at 0.1 Hz and evoked responses averaged for each site separately. When 2 neocortical sites were stimulated during the induction phase, the stimuli were either applied at the same time or, as a control, separated by a delay of 65 ms. In other control experiments, the stimulation intensity at the paired sites was reduced by decreasing the shock durations from 300 to 100 μs during induction.

Drugs

Lidocaine and the NMDA receptor antagonist 2-amino-5-phosphonopentanoic acid (AP5) were obtained from Sigma-Aldrich (St. Louis, MO), whereas the group I metabotropic glutamate receptor (mGluR) antagonist 1-aminoindan-1,5-dicarboxylic acid (AIDA) was obtained from Tocris Bioscience (Ellisville, MO). All drugs were dissolved in artificial cerebrospinal fluid (aCSF). However, whereas lidocaine (4%) was microinfused in area 36 or the adjacent ventral association neocortex, AP5 (100 μM) and AIDA (100 μM) were applied via the arterial perfusate for 12 min in the absence of stimulation. We focused on the role of NMDA and group I metabotropic receptors because earlier in vitro studies on activity-dependent plasticity in the perirhinal cortex have implicated these receptors in the induction of perirhinal LTP and long-term depression (LTD) (Bilkey 1996; Ziakopoulos et al. 1999; Cho et al. 2000, 2001; Jo et al. 2008).

Lidocaine Microinfusions

In these experiments, 4 concentric stimulating electrodes were positioned along the rostrocaudal axis of area 36 or in the adjacent neocortex. These electrodes could be used to deliver electrical stimuli or record field potentials. In between the 2 most rostral and caudal concentric electrodes, along 2 closely spaced (1 mm) microsyringe penetrations, we made multiple small infusions of either vehicle (total volume of 0.8 μL of aCSF) or lidocaine (total volume of 0.8 μL of 4% lidocaine in aCSF) across the cortical thickness (0.5 μL/min). Prior to the infusions, after positioning the electrodes and microsyringe, 10 electrical stimuli (100 μs, 0.5 mA; 0.1 Hz) were applied at stimulation sites of interest (as specified in the results section) and evoked responses averaged for each site separately. The infusions were then performed. Five, 30, and 60 min after concluding the infusions, we again obtained independent averages of the responses elicited by the same stimulation sites as in the preinfusion phase.

Data Analysis

All field potentials and optical responses depicted in this study are averages of 10 stimuli applied 10 s apart. Because neocortically evoked unit discharges usually occurred after the negative peak of the field response (during the rising phase of the subsequent positivity), our field potential measurements (slope and amplitude) focused on the voltage difference between the negative and positive peaks. However, because TFS caused qualitatively identical changes in response slope and amplitude, for simplicity, the Results section only reports percent changes in amplitudes. For optical recordings, we identified square regions of interest centered on each field recording electrode and averaged the fluorescence signal in all the pixels they included. In all cases, these regions of interest measured around 17 by 17 pixels, corresponding to a surface of 886 by 886 μm. Within these regions, the average delta F/F was determined and compared across 3 time points: preinduction (control), as well as 5 and 30 min postinduction. All data are expressed as means ± standard errors.

Histology

At the conclusion of the experiments, the brains were removed from the recording chamber and placed in a fixative containing 2% paraformaldehyde and 1% glutaraldehyde for at least 1 week. The brains were then sectioned on a vibrating microtome (at 100 μm) and stained with cresyl violet to determine the position of recording and stimulating sites. All the data reported below was obtained in cases where both the stimulating and recording electrodes had reached their intended location (see example of histological control in Fig. 1*C*).

Results

Field Potentials and Optical Signals Evoked by Neocortical Stimuli in Perirhinal Area 36

As previously described in the isolated guinea pig brain in vitro preparation (Biella et al. 2001, 2002), neocortical stimuli typically evoked biphasic field potential responses in layer III of area 36 (Fig. 2*A2*,*B2*). These responses consisted of an initial negativity followed by positive component. Several observations indicate that these field potentials are generated locally (e.g., not volume conducted from a distant site). First, their latency became longer

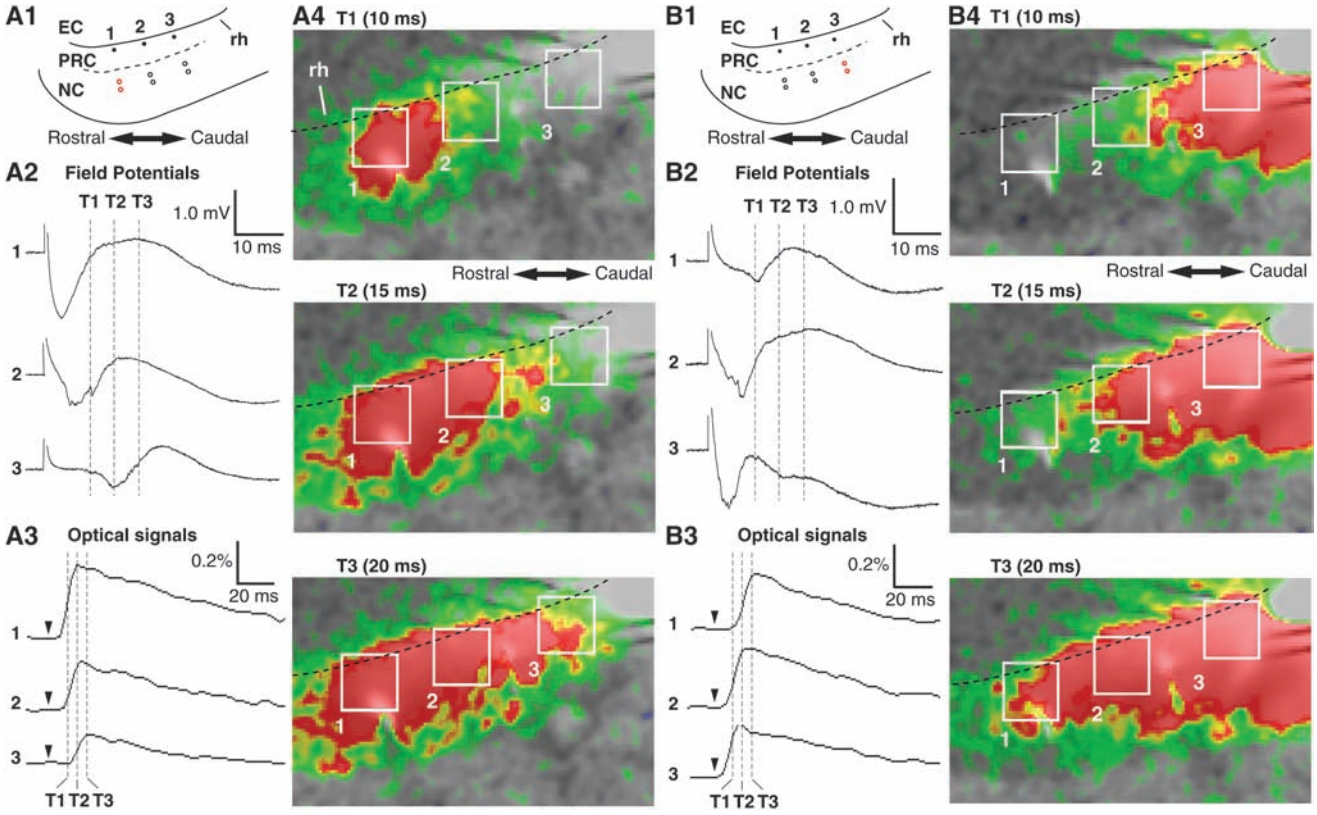

Figure 2. Area 36 responses to neocortical stimulation as measured with field potentials and optical measurements of voltage-sensitive signals. Panels *A* and *B* show area 36 responses to electrical stimuli delivered at the most anterior or posterior neocortical stimulation sites, respectively. The schemes in panels 1 show the stimulation (red) and recording sites. These neocortical stimuli elicited field potential (2) and optical responses (3–4). Panel 3 plots the fluorescence in all pixels included in the 3 square regions shown in panel 4 as a function of time. Arrowheads indicate when the stimulus was applied. The dashed vertical lines labeled T1–3 in 2 and 3 coincide in time. Panel 4 shows time-lapsed pictures of optical signals elicited by neocortical stimuli at the times indicated by the dashed vertical lines T1–3.

as the rostrocaudal distance between the stimulating and recording sites increased. For instance, panels A2 and B2 of Figure 2 illustrate field potential responses elicited from the rostral-most (Fig. 2*A*1, red circles) and caudal-most (Fig. 2*B*1, red circles) neocortical stimulation sites, respectively. Note that in both cases, the latency of the evoked field potential was shortest at the perirhinal level adjacent to the stimulation site and that it increased with the distance between the stimulation and recording sites. In addition, the amplitude of responses in the perirhinal cortex generally decreased with rostrocaudal distance from the stimulation site. Compared with the field potential responses seen at the perirhinal site in transverse register with the stimulation site, response amplitudes decreased 17 ± 8% and 57 ± 7% at the intermediate and most distant recording sites, respectively (paired *t*-tests, $P = 0.006$ and 0.00005, $n = 30$).

Second, the rostrocaudal propagation of simultaneously recorded optical signals followed a similar time course to that of evoked field potentials. An example of this is shown in Figure 2*A*4,*B*4. Examination of the time-lapsed color-coded images of the optical signal intensity reveals that when neocortical stimuli were delivered rostrally (Fig. 2*A*4), the optical signal appeared first rostrally in area 36 and then propagated caudally. Conversely, when the stimuli were applied at the caudal neocortical site (Fig. 2*B*4), the posterior part of area 36 was activated first and the signal then propagated rostrally. Furthermore, when we integrated the optical signals generated close to the recording electrodes (Fig. 2*A*3,*B*3) and compared their latency with that of the field potentials picked up by the same electrodes (Fig. 2*A*2,*B*2), a parallel was observed between the 2 measures. This can be seen by comparing the position of the dashed vertical lines at the 3 sites in panels 2 (field potentials) and 3 (optical signals) of Figure 2*A*,*B*.

In addition to the close parallel between the time-dependent propagation of field potential and optical responses, the local origin of the field potential responses was indicated by the fact that neocortical stimuli could often be seen to evoke orthodromic discharges in layer III area 36 neurons. As shown in the representative examples of Figure 3, these orthodromic responses typically occurred during the rising phase of the positive component of the field potentials recorded at the same site by the same microelectrode (for population analysis of latencies, see inset in Fig. 3*B*). However, it should be noted that in the experiments described below, we purposefully avoided recording unit responses because they distorted the field potentials, complicating the analysis of activity-dependent changes in neocortically evoked activity.

In closing this section, it should be noted that to our surprise, neocortical stimuli, whether delivered at 1 site or 2 sites simultaneously, failed to elicit significant optical signals in the entorhinal cortex, even when delivered at a high frequency. This observation is consistent with earlier reports in the isolated guinea pig brain from de Curtis and colleagues (Biella et al. 2001, 2002, 2003, 2010) where it was shown that neocortical or area 36 stimuli elicit no local field responses or optical signals in the entorhinal cortex. In contrast, stimulation of the olfactory tract

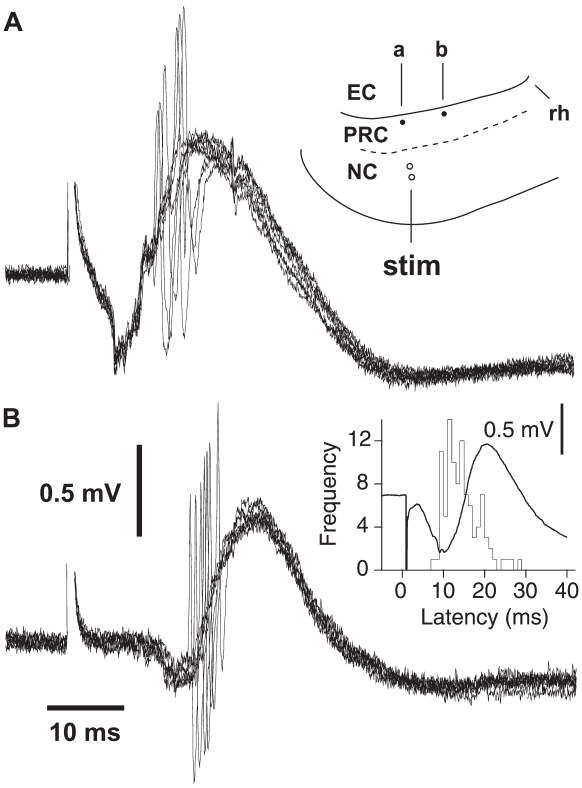

Figure 3. Neocortical stimuli elicit orthodromic responses in area 36 neurons. *A* and *B* show representative examples of single-unit orthodromic responses elicited in area 36 neurons by neocortical stimuli. Each panel shows 8 superimposed responses. The evoked signal was not filtered to allow examination of the temporal relationship between the evoked field potentials and unit activity. The recording and stimulation sites are indicated in the scheme shown as an inset in panel *A*. Inset in panel *B* shows the frequency distribution of median orthodromic response latencies in 102 area 36 neurons. To correct for changes in response latencies related to the varying distance between neocortical stimulation sites and perirhinal recording sites, all data was aligned in time to the negative peak of the evoked field potentials.

or hippocampus in the same preparation could elicit large optical signals and field responses in the entorhinal cortex (Gnatkovsky et al. 2004; Uva and de Curtis 2005; Gnatkovsky and de Curtis 2006). Since the perirhinal cortex sends strong projections to the entorhinal cortex (reviewed in Witter et al. 2000), the lack of optical responses in the entorhinal cortex following perirhinal stimuli implies that perirhinal to entorhinal communication is regulated by strong feed-forward inhibition (de Curtis and Pare 2004).

Effect of TFS at a Single Neocortical Stimulation Site in Area 36

To study activity-dependent changes produced by neocortical inputs in area 36, we first tested the effects of TFS applied at a single neocortical stimulation site on simultaneously recorded field potentials and optical signals (n = 12). Across these experiments, each of the 3 neocortical stimulation sites served as induction site an equal number of times. These experiments consisted of 3 phases: 1) a control phase where 10 stimuli were delivered at each of the 3 neocortical sites independently at a low frequency and evoked responses averaged; 2) an induction phase where a randomly selected neocortical stimulation site received TFS while the other 2 sites were left unstimulated; and 3) a postinduction phase where 5 and 30 min later, stimuli were delivered independently at the 3 neocortical sites at a low frequency as in the control phase.

Irrespective of the induction site, TFS caused a robust and long-lasting depression of the responses evoked by the induction site leaving the responses evoked by the 2 control sites unchanged. This depression was global in that it was observed at all recording sites and could be observed in both the field potentials and optical signals. A representative example of this phenomenon is shown in Figure 4. In this experiment, the most rostral and caudal neocortical stimulation sites (respectively, panels 1 and 3 of Fig. 4*A–C*) served as controls whereas the third site (panels 2 of Fig. 4*A–C*) received TFS. Both optical signals (Fig. 4*A*2,*B*2) and field potentials (Fig. 4*C*2) evoked from the induction site were significantly reduced (30-min test: field potential to 82.0 ± 0.3% of baseline, t-tests, $P < 0.05$). Although some response variations were seen at the control sites, these effects proved nonsignificant across experiments as they were of much smaller magnitude and inconsistent polarity (see below).

Across experiments, a repeated measures analysis of variance (ANOVA) on the amplitude of field potential responses revealed a significant effect of time ($F_{2,58}$ = 12.37, $P <$ 0.0001) and stimulation sites ($F_{1,58}$ = 15.521, P = 0.0005) plus a significant interaction between the 2 ($F_{2,58}$ = 5.388, P = 0.007). Similar results were obtained with the optical signals (time, F = 10.092, P = 0.0002; stimulation site, F = 10.43, P = 0.002; interaction, F = 9.52, P = 0.003). Bonferroni-corrected post hoc t-tests confirmed that the field potentials elicited from the induction sites were significantly reduced compared with control sites (t-tests, P = 0.0003, n = 12) to 65.8 ± 6.3% and 68.7 ± 7.1% of baseline at the 5 and 30 min tests, respectively (Fig. 6*A*1, squares). Similar results were obtained for optical responses (t-tests, $P < 0.0001$): reduction to 56.8 ± 8.8% and 73.1 ± 9.9% of baseline at the 5 and 30 min tests, respectively (Fig. 6*B*1, squares). Optical and field potential responses evoked from the control sites were unchanged (t-tests, $P >$ 0.2 for all tests) at both the 5 min (103.1 ± 5.4% and 91.1 ± 4.5%) and 30 min postinduction tests (94.8 ± 4.6% and 95.1 ± 5.2%; Fig. 6*A*2,*B*2, squares).

Effect of Paired Theta-Frequency Neocortical Stimulation in Area 36

To test whether the perirhinal network allows for associative plasticity, we next tested the effects of TFS applied simultaneously at 2 different neocortical sites on simultaneously recorded field potentials and optical signals. The control and postinduction phases were exactly as above. However, in the induction phase, 2 of the 3 neocortical sites received TFS while the third was left unstimulated and served as a control.

Irrespective of the particular combination of sites selected for TFS, this induction paradigm caused a long-lasting potentiation of responses evoked from the paired induction sites leaving the responses evoked from the control sites unchanged (n = 9). As for the response depression described above, this potentiation was global in that it affected all recording sites and could be observed in both the field potentials and optical responses.

A representative example of these observations is illustrated in Figure 5. In this case, the most rostral and caudal stimulation sites (respectively, panels 1 and 3 of Fig. 5) received paired TFS whereas the third site (panels 2 of Fig. 5) was unstimulated

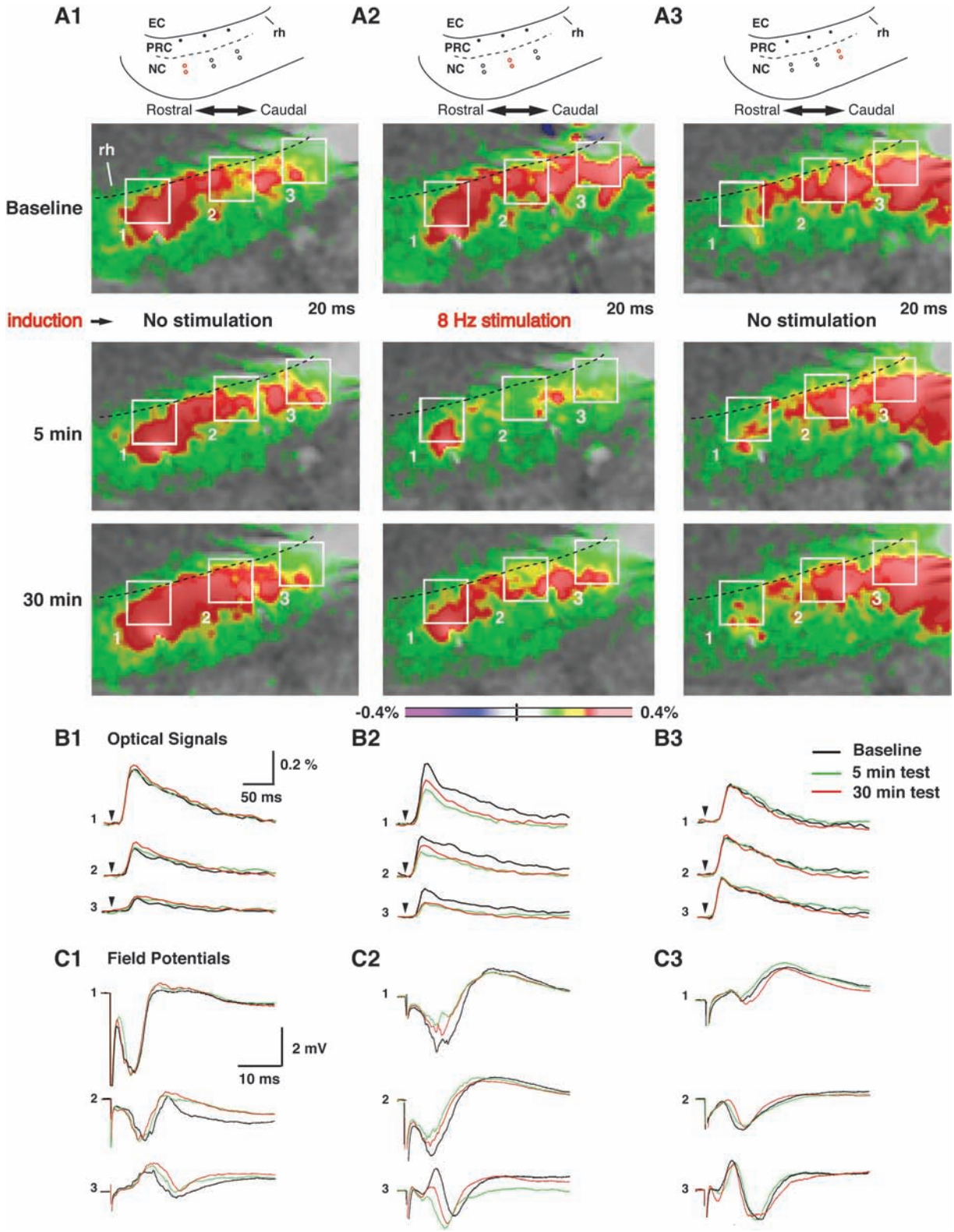

Figure 4. TFS at a single neocortical stimulation site produces a long-lasting and site-specific depression of evoked responses. (*A*1–3) Electrical stimuli were delivered in the neocortex at the sites indicated by red circles in the schemes (top). In the control phase (Baseline), single shocks were delivered at each site independently. During the induction phase, one of the sites (*A*2) received TFS (8 Hz stimulation) while the others were not stimulated. Five and 30 min later, single shocks were delivered at all sites independently. The pictures in *A* show optical signals generated by the 3 neocortical stimuli (20 ms after the stimuli) during the control phases (top) as well as 5 (middle) and 30 min (bottom) after TFS. *B* plots the fluorescence in all pixels included in the 3 square regions shown in the pictures of panel *A*. Arrowheads indicate when the stimulus was applied. *C* shows the field potential responses elicited by the neocortical stimuli. In *B* and *C*, the black, green, and red lines indicate activity obtained during the control phase, as well as 5 and 30 min after TFS, respectively.

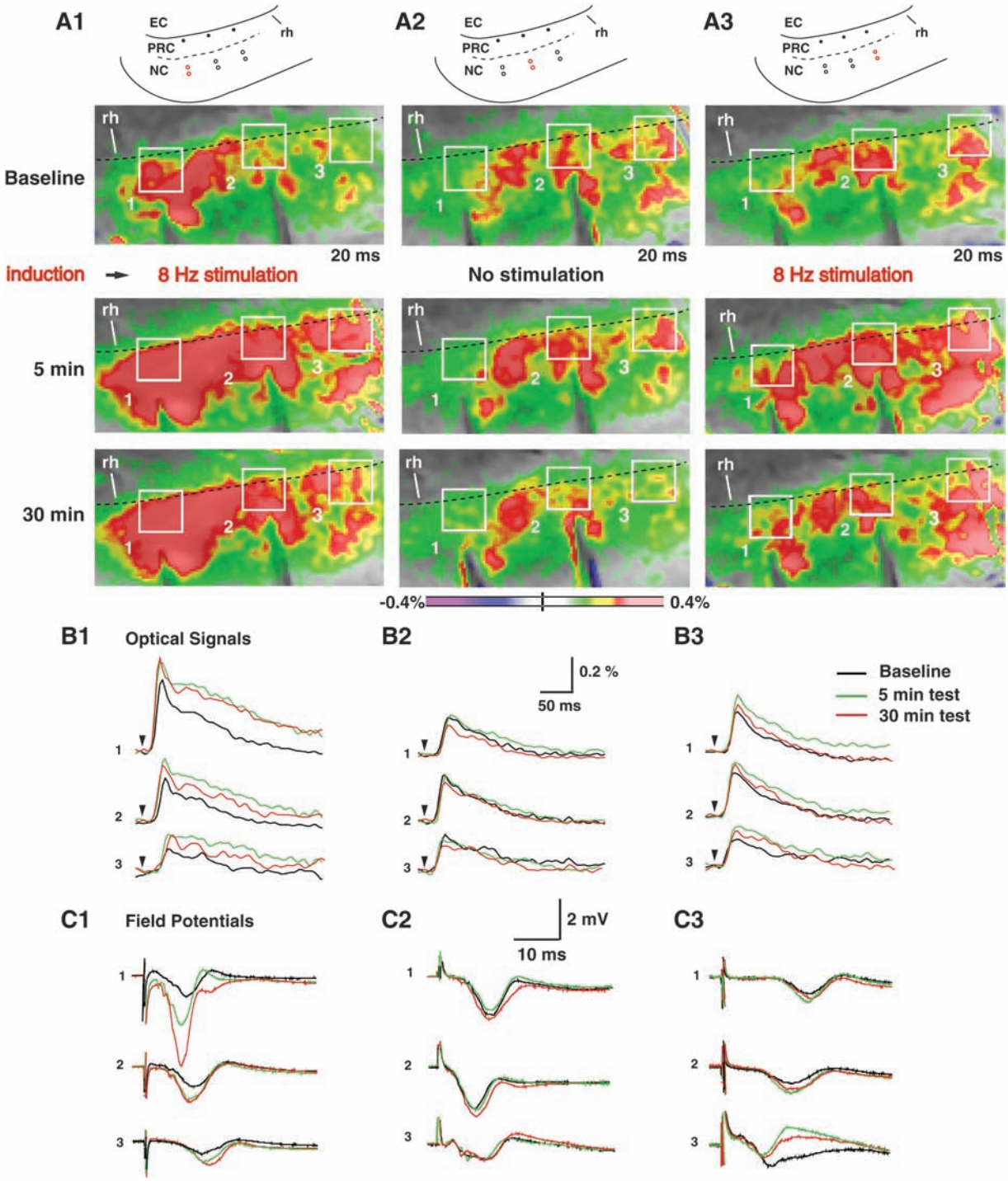

Figure 5. TFS at 2 neocortical stimulation sites produces a long-lasting potentiation of responses evoked by the paired sites. (*A*1–3) Electrical stimuli were delivered in the neocortex at the sites indicated by red circles in the schemes (top). In the control phase (Baseline), single shocks were delivered at each site independently. During the induction phase, 2 of the sites (*A*1, *A*3, red circles) received TFS (8 Hz stimulation) while the third (*A*2, red circles) was not stimulated. Five and 30 min later, single shocks were delivered at all sites independently. The pictures in *A* show optical signals generated by the 3 neocortical stimuli (20 ms after the stimuli) during the control phases (top) as well as 5 (middle) and 30 min (bottom) after TFS. *B* plots the fluorescence in all pixels included in the 3 square regions shown in the pictures of panel *A*. Arrowheads indicate when the stimulus was applied. *C* shows the field potential responses elicited by the neocortical stimuli. In *B* and *C*, the black, green, and red lines indicate activity obtained during the control phase, as well as 5 and 30 min after TFS, respectively.

during induction. Both optical signals (Fig. 5*A*1,*A*3,*B*1,*B*3) and field potentials (Fig. 5*C*1,*C*3) evoked from the induction sites were significantly enhanced (30-min test: field potential enhanced to 330 ± 2% of baseline for the rostral site; to 211 ± 3% of baseline for the caudal site, *t*-tests, $P < 0.05$). Response variations at the control sites proved nonsignificant across experiments as they were of much smaller magnitude and inconsistent polarity (see below).

Across experiments, a repeated measures ANOVA on the optical signals revealed a significant effect of time ($F_{2,86} = 6.42$,

$P = 0.002$) and stimulation sites ($F_{1,86} = 14.29$, $P = 0.0005$) plus a significant interaction between the two ($F_{2,86} = 10.2$, $P = 0.0001$). Bonferroni-corrected post hoc *t*-tests confirmed that optical responses elicited from the induction sites were significantly enhanced relative to those evoked from control sites ($P < 0.0001$, $n = 9$) to 146.4 ± 7.7% and 131.1 ± 8.7% of baseline at the 5- and 30-min tests, respectively (Fig. 6*B*1, circles). Similarly, paired TFS caused a persistent and significant increase in field potential responses evoked from the induction sites (142.6 ± 13.5% of baseline at the 30-min test; paired *t*-test, $P = 0.021$; Fig. 6*A*1, circles). In contrast, optical and field potential responses evoked from the control site were unchanged (*t*-tests, $P > 0.1$ for all tests) at both the 5-min (99.0 ± 4.2% and 99.5 ± 3.5%) and 30-min tests (93.5 ± 5.2% and 91.8 ± 8.0%; Fig. 6*A*2,*B*2, circles).

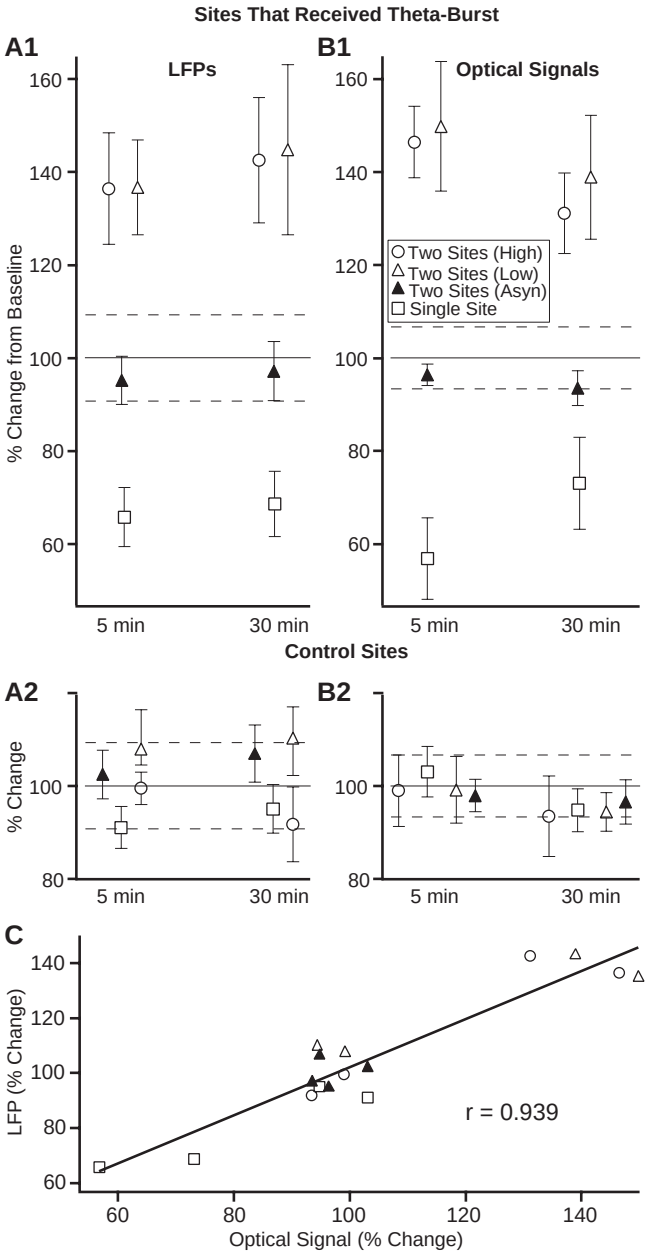

Figure 6. Site-specific effects of TFS in the various conditions tested in the present study. Percent change in field potential (*A*) and optical (*B*) response amplitudes (*y*-axis, normalized to baseline) seen at the sites that received TFS (1) or acted as controls (2), 5 and 30 min (*x*-axis) after induction across all experiments. Dashed lines indicate standard error of the baseline condition where the greatest variability was observed. Different symbols are used to represent data obtained in the different conditions investigated: empty squares, TFS applied at a single neocortical site; empty circles, TFS "simultaneously" applied at 2 neocortical sites; empty triangles, low-intensity TFS applied simultaneously at 2 neocortical stimulation sites; solid triangles, TFS applied "asynchronously" (65 ms delay) at 2 neocortical stimulation sites. (*C*) Correlation between changes in response amplitudes seen in the various conditions investigated in this study, as measured with local field potentials (*y*-axis) and optical signals (*x*-axis).

Impact of Stimulation Intensity on the Effect of Paired TFS

In the above experiments, it could be argued that the contrasting effects of TFS applied at 1 versus 2 neocortical sites might only reflect differences in the intensity of stimulation during induction. To test if this was the case, we repeated the paired TFS experiments except that during induction, the stimulation intensity was lowered by reducing the stimulus duration to 33% of those used in the above set of experiments. In other words, all aspects of the protocol were unchanged except for a drastically lower simulation intensity during the induction phase. In separate experiments, we determined that lowering the neocortical stimulus duration caused a large and significant reduction in the amplitude of evoked field potential responses in the perirhinal cortex (–58 ± 12% of baseline, $n = 19$; paired *t*-test, $P = 0.0001$).

Remarkably, qualitatively identical results were obtained with the lower stimulation intensity (Fig. 6, empty triangles). That is, the responses evoked from the induction sites showed as much potentiation as with the higher stimulation intensity relative to those evoked from the unstimulated sites ($n = 9$). Across experiments, a repeated measures ANOVA on the optical signals revealed a significant effect of time ($F_{2,68} = 3.82$, $P = 0.027$) and stimulation sites ($F_{1,68} = 6.54$, $P = 0.015$) plus a significant interaction between the two ($F_{2,68} = 4.65$, $P = 0.012$). Bonferroni-corrected post hoc *t*-tests confirmed that optical responses elicited from the induction sites were significantly enhanced relative to those evoked from control sites ($P < 0.0017$, $n = 9$) to 149.8 ± 13.9% and 138.9 ± 13.3% of baseline at the 5- and 30-min tests, respectively (Fig. 6*B*1, empty triangles). Similarly, paired low-intensity TFS caused a persistent and significant increase in field potential responses evoked from the induction sites (143.3 ± 18.2% of baseline at the 30-min test; paired *t*-test, $P = 0.036$; Fig. 6*A*1, empty triangles). In contrast, optical and field potential responses evoked from the control site were unchanged (*t*-tests, $P > 0.1$ for all tests) at both the 5-min (99.2 ± 7.2% and 107.9 ± 8.4%) and 30-min tests (94.4 ± 45.1% and 110.3 ± 6.7%; Fig. 6*A*2,*B*2, empty triangles).

Impact of Input Timing on the Effect of Paired TFS

In the above experiments, it is unclear whether the response potentiation caused by paired TFS required strict coincidence of the stimuli during induction. Thus, to address this question, we next examined whether delaying 1 of the 2 inputs by half a theta cycle affected the response potentiation at the induction sites compared with those evoked from the control sites ($n = 12$). Note that the duration of this offset (65 ms) is roughly 4–5 times longer than the time required for neocortical inputs to propagate through the full rostrocaudal extent of the perirhinal cortex.

Whether we considered optical or field potential responses, asynchronous TFS caused no change in response amplitudes at

the induction and the control stimulation sites. This was true for comparisons of field potential responses at the induction (baseline vs. 30 min postinduction: paired *t*-test, $P = 0.23$) and control stimulation sites (baseline vs. 30-min postinduction: paired *t*-test, $P = 0.35$) as well as for optical signals (baseline vs. 30-min postinduction: induction sites, $P = 0.13$; control sites, $P = 0.49$). The average data obtained in these experiments is shown in Figure 6*A*,*B* (solid triangles).

Across the various conditions investigated above, a near perfect correlation was found between the activity-dependent shifts in response amplitudes as assessed with field potentials and optical signals ($r = 0.939$; Fig. 6*C*).

Network Mechanisms Underlying the Contrasting Effects of TFS at 1 Versus 2 Distant Neocortical Sites

Overall, the above suggests that convergence of pathways conveying short- and long-range neocortical influences on the same perirhinal neurons during TFS is important for the induction of activity-dependent potentiation. However, the trajectory of the pathways involved remains unidentified. In an earlier study performed on horizontal slices of the perirhinal cortex, it was found that knife cuts in the perirhinal cortex, but not the adjacent neocortex, abolished the longitudinal propagation (Martina et al. 2001). However, it is conceivable that in the intact network of the whole brain, the situation is different. Indeed, if neocortical axons en route to the perirhinal cortex curve out of the plane of the horizontal slice, knife cuts would have no effect since the axons are already interrupted when the brain is sectioned to prepare horizontal slices. In contrast, in the intact network of the whole brain, such sinuous axons are preserved and their contribution can be tested.

To address this question, we studied the impact of local infusions of lidocaine in the perirhinal cortex or adjacent temporal neocortex. A difficulty in these experiments is to determine a volume and concentration of lidocaine that is sufficient to interfere with propagation while having only local effects (i.e., little spread from the infusion site). We are thus forced into a compromise between these 2 requirements. To address this, we first performed control experiments where we examined how various amounts of lidocaine infused in the perirhinal cortex affected responses elicited by direct stimulation of the perirhinal cortex itself. Lidocaine was infused at mid rostrocaudal levels of the perirhinal cortex with 2 concentric electrodes on either side of the infusion site, as shown in Figure 7*A*1. These electrodes could be used to both record and stimulate the perirhinal cortex. By trial and error, and guided by earlier studies on lidocaine diffusion in cerebral tissue (Tehovnik and Sommer 1997; Broadbent et al. 2006; Fujita et al. 2010), we determined that a total volume of 0.8 μL of lidocaine (4%) divided in multiple small infusions along 2 microsyringe penetrations (Fig. 7*A*1, red asterisks) could produce a significant reduction of longitudinal propagation with little spread from the infusion site. Moreover, with these parameters, we found that the lidocaine effects dissipated within 60 min.

Figure 7*A*2 shows a representative example of this experiment. Here, we contrast responses evoked and recorded from sites either rostral or caudal to the lidocaine infusion site (close sites) versus cases where the infusion site was in between the stimulation and recording sites (distant sites). Prior to the infusion, when perirhinal electrode 4 was stimulated, field responses were observed at recording sites 1–3 (baseline, black traces). Thirty minutes after the lidocaine infusion (red traces), responses recorded at the close site (3) were unchanged. In contrast, at distant sites (electrodes 1 and 2), a large response reduction was observed. One hour after the lidocaine infusion, all responses retuned to baseline level.

As shown in Figure 7*A*3, these effects were consistent across multiple experiments. Here, we plot normalized fluctuations in response amplitude as a function of time from infusion of lidocaine (empty symbols, $n = 8$) or vehicle (filled symbols, $n = 8$) at close (circles) and distant (triangles) sites. As visually evident, compared with the vehicle experiments, the only significant reduction caused by perirhinal lidocaine infusions were seen at distant sites, when the lidocaine was infused in between the stimulation and recording sites. This effect was seen 5- and 30-min postinfusion (5 min, 61.4 ± 3.6% of baseline, *t*-test, $P < 0.0001$; 30 min, 66.1 ± 4.2%, *t*-test, $P < 0.0001$) and had vanished 60 min postinfusion (90.5 ± 0.8%, *t*-test, $P = 0.3201$).

Next, we examined how the same amount of lidocaine infused in the temporal neocortex (Fig. 7*B*) or adjacent perirhinal cortex (Fig. 7*C*) affected the longitudinal propagation of neocortical inputs in the perirhinal cortex. With neocortical infusions of lidocaine (Fig. 7*B*1), no reduction in longitudinal propagation was observed. That is, perirhinal field potential responses at sites rostrocaudally distant from the neocortical stimulation sites were not significantly reduced ($n = 8$; Fig. 7*B*2). In contrast, when lidocaine was infused at the same rostrocaudal level but in the perirhinal cortex (Fig. 7*C*1), a large and significant reduction in response amplitude was seen at perirhinal sites rostrocaudally distant from the neocortical simulation site (Fig. 7*C*2, triangles) with no difference in response amplitudes at the close perirhinal sites (Fig. 7*C*2, circles). These contrasting effects of neocortical and perirhinal infusions of lidocaine strongly suggest that a large portion of the axons conveying long-range neocortical influences course in the perirhinal cortex itself, not in the adjacent temporal neocortex.

Last, we tested the effects of perirhinal infusion of lidocaine on the activity-dependent plasticity produced by TFS at 1 (Fig. 8*A*) versus 2 distant neocortical stimulation sites (Fig. 8*B*). In all cases, TFS was applied 5 min after finishing the lidocaine injection, and the impact of this manipulation was assessed 60 min later, when our control experiments had revealed that the lidocaine effects had dissipated. With TFS application at a single neocortical stimulation site, contrasting results were obtained depending on the position of the recording site with respect to the lidocaine infusion site (Fig. 8*A*1). When lidocaine was infused in between the recording and stimulation site (Fig. 8*A*2, Distant sites), TFS at one neocortical site produced no significant change in response amplitude (91.8 ± 6.7% of baseline, *t*-test, $P = 0.61$), compared with a significant reduction in controls (76.1 ± 10.2% of baseline, *t*-test, $P = 0.0003$). In contrast, at close recording sites, a –48.4 ± 12.2% reduction in response amplitude was seen, statistically indistinguishable from the depression seen in controls (48.9 ± 21.9% of baseline, *t*-test, $P = 0.32$). When TFS was applied simultaneously at 2 distant neocortical sites after perirhinal infusions of lidocaine, instead of the ubiquitous potentiation observed in control cases (Fig. 8*B*2, empty bars), we observed a significant response depression at close sites (–26.1 ± 5.9%, *t*-test, $P = 0.03$) and the same trend at distant sites. Overall, these results point to a critical role of longitudinal perirhinal pathways in the induction of activity-dependent plasticity of neocortical inputs in the perirhinal cortex.

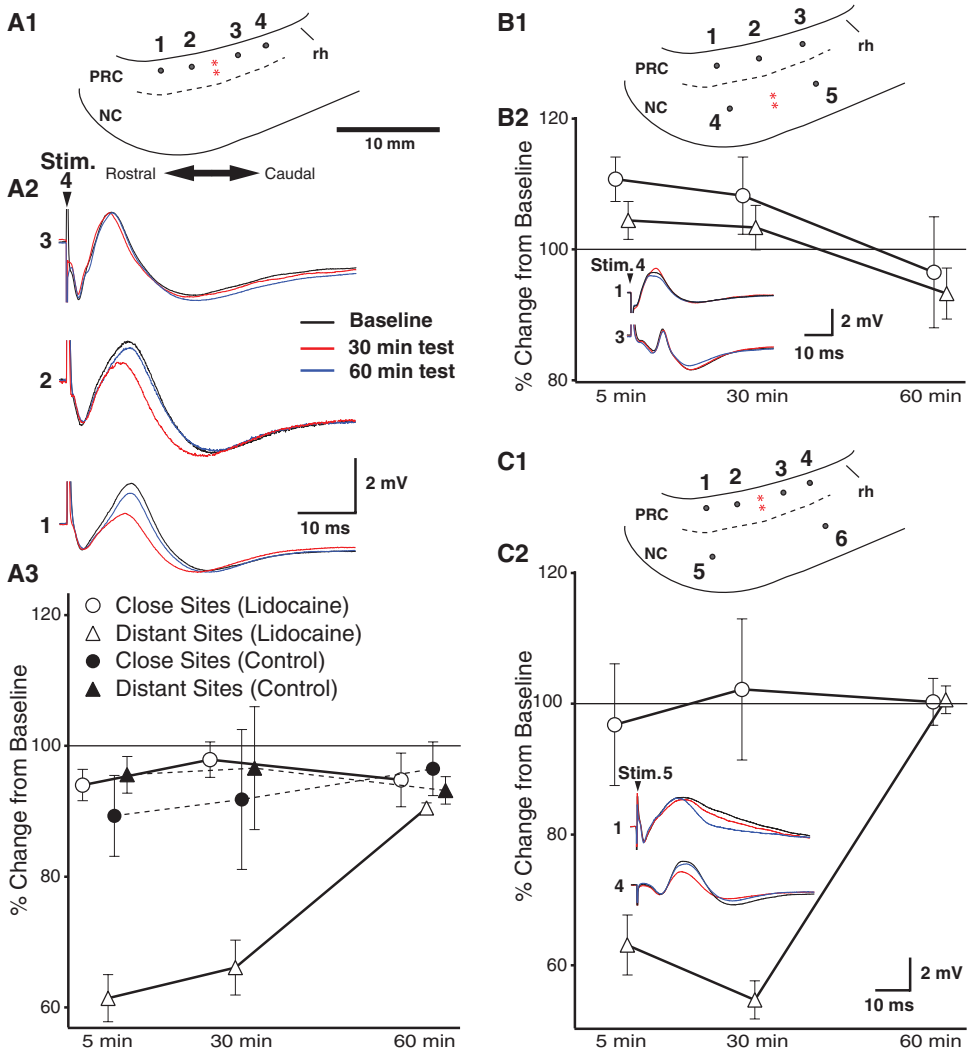

Figure 7. Differential impact of local lidocaine infusions in area 36 or the ventral temporal neocortex. The results of 3 series of experiments (*A*–*C*) are shown. The schemes in panels 1 contrast the position of concentric electrodes (filled circles) and lidocaine infusions (red asterisks) used in each of these experiments. (*A*) Control experiments to assess lidocaine diffusion versus a similar volume of vehicle. In this case, we stimulated and recorded in the perirhinal cortex (*A*1). (*A*2) Field responses elicited at sites 3, 2, and 1 by electrical stimuli delivered through perirhinal electrode 4 (black, baseline; red and blue, 30 and 60 min postlidocaine infusion, respectively). (*A*3) Average of results obtained in 8 such lidocaine and 8 vehicle experiments. (*B*) Impact of neocortical lidocaine infusion on perirhinal responses to neocortical stimuli. (*B*1) Electrode configuration and lidocaine infusion sites. (*B*2) Average of all experiments combined (% change in field potential responses from baseline at close and distant sites; $n = 8$). Inset in *B*2 shows a representative experiment where lidocaine was infused in the temporal neocortex. (*C*) Impact of perirhinal lidocaine infusion on perirhinal responses to neocortical stimuli. (*C*1) Electrode configuration and lidocaine infusion sites. (*C*2) Average of all experiments combined (% change in field potential responses from baseline at close and distant sites; $n = 8$). Inset in *C*2 shows a representative experiment where lidocaine was infused in the perirhinal cortex.

Dependence of Activity-Dependent Plasticity on Group I Metabotropic Glutamate and NMDA Receptors

Finally, we examined the induction mechanisms of the LTD and LTP described above. Earlier in vitro brain slice studies have implicated the activation of NMDA and group I mGluRs in the induction of perirhinal LTP and LTD (Bilkey 1996; Ziakopoulos et al. 1999; Cho et al. 2000, 2001; Jo et al. 2008). Therefore, we examined the effects of the NMDA receptor antagonist AP5 (100 μM) and of the group I mGluR antagonist AIDA (100 μM). In all the experiments described below, the drugs were applied separately for 12 min via the arterial perfusate, the control and test responses were measured while perfusing the brain with the control perfusate, and the test phase occurred 30 min after returning to the control perfusate.

Since we aimed to test whether NMDA or group I mGluR activation during TFS was required for LTP or LTD induction, it was critical to first determine whether AP5 or AIDA application, in the absence of TFS, affected response amplitudes beyond the period of drug application. Thus, after obtaining a baseline measure of response amplitudes with the control perfusate, we applied AP5 ($n = 5$) or AIDA ($n = 5$) for 12 min in the absence of neocortical stimuli and measured response amplitudes again, 30 min after returning to the control perfusate. No significant changes in response amplitudes were detected in these control experiments (Fig. 9*A*; paired *t*-tests, $P \geqslant 0.45$; AP5, -3.6 ± 3.2%; AIDA, 4.4 ± 3.7%).

Next, we tested whether application of the same drugs during TFS at 1 or 2 neocortical sites interfered with LTD or LTP induction, respectively. We first compared the effects of TFS applied at one neocortical site (Fig. 9*B*) on perirhinal field potential response amplitudes in control conditions ($n = 12$) versus in the presence of AP5 ($n = 15$) or AIDA ($n = 15$). While

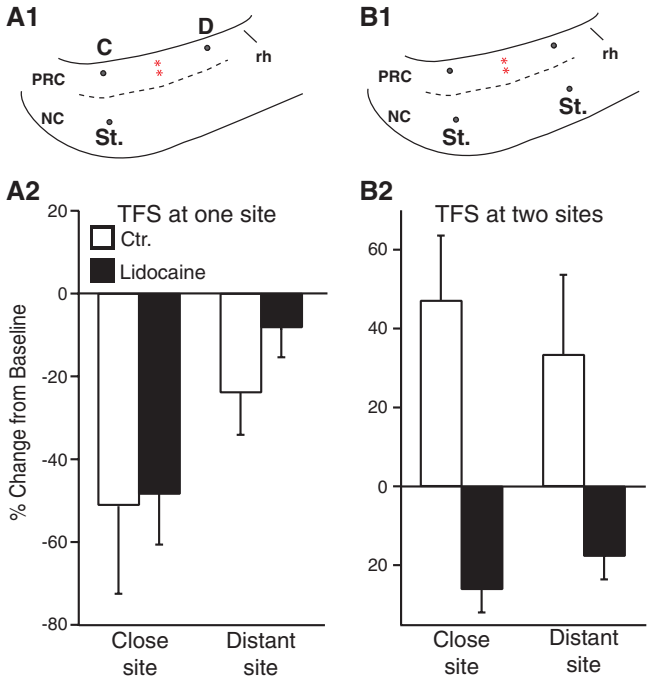

Figure 8. Impact of lidocaine infusion in the perirhinal cortex on activity-dependent modification of neocortical responses induced by TFS applied at 1 (*A*) or 2 (*B*) neocortical stimulation sites. The schemes in the top panels illustrate the relative position of neocortical stimulating (St.) and area 36 recording electrodes (dots) located at proximity (C for close) or at a distance (D) from the stimulation site. Red asterisks mark the lidocaine infusion sites in area 36. (*A*1) TFS at one neocortical stimulation site. (*B*1) TFS at 2 neocortical stimulation sites. In this case, depending on the stimulating electrode considered, the same area 36 recording site was termed a close or distant site, hence the absence of C and D labels. After measurement of baseline response amplitudes, the same amount of lidocaine as in Figure 7*C*1 was infused at mid rostrocaudal perirhinal levels (red asterisks). Five minutes after concluding the infusion, TFS was applied at 1 (*A*) or 2 (*B*) neocortical stimulation sites. Panels 2 impact of neocortical TFS was then assessed after the lidocaine effect had dissipated (60-min postinfusion). Filled and empty bars show the results obtained in lidocaine and control experiments, at perirhinal recording sites close to (i.e., in rostrocaudal register) the neocortical induction sites or at distant sites ($n = 8$).

AP5 did not prevent the depression of responses evoked from the induction site (Fig. 9*B*, control vs. AP5, *t*-test, $P = 0.95$), application of AIDA transformed the depression seen in control conditions into a potentiation (Fig. 9*B*; control vs. AIDA, *t*-test, $P = 0.0002$).

Last, we compared the effects of TFS applied simultaneously at 2 distant neocortical stimulation sites (Fig. 9*C*) on perirhinal field potential response amplitudes in control conditions ($n = 9$) versus in the presence of AP5 ($n = 10$) or AIDA ($n = 10$). Addition of AP5 to the arterial perfusate during LTP induction transformed the potentiation of responses evoked from the induction sites into a depression (Fig. 9*C*; control vs. AP5, *t*-test, $P = 0.0016$). In contrast, application of AIDA did not prevent the response potentiation (Fig. 9*C*; control vs. AIDA, *t*-test, $P = 0.62$). In the above AP5 and AIDA experiments, whether TFS was applied at 1 or 2 sites, responses elicited from the control neocortical stimulation sites did not change significantly.

Discussion

The present study was undertaken to test whether the perirhinal network allows for associative synaptic plasticity between coincident but spatially distributed neocortical activation patterns. The interest of this question stems from earlier findings indicating that the perirhinal cortex plays a critical role in high-order perceptual functions as well as in recognition and associative memory in various sensory modalities (Zola-Morgan et al. 1989, 1993; Bunsey and Eichenbaum 1993; Meunier et al. 1993, 1996; Suzuki et al. 1993; Eacott et al. 1994; Mumby and Pinel 1994; Higuchi and Miyashita 1996; Herzog and Otto 1997; Buckley and Gaffan 1998). Here, we found that repeated activation of focal versus distributed neocortical inputs elicited long-term changes in perirhinal responsiveness of opposing polarities (depression vs. potentiation, respectively). These long-term changes in perirhinal responsiveness to the repeatedly activated neocortical inputs were global in that they were observed at all rostrocaudal levels of area 36. Moreover, lidocaine microinfusion experiments revealed that longitudinal pathways coursing in the perirhinal cortex itself (not in the adjacent ventral association temporal neocortex) played a critical role in the induction of activity-dependent plasticity. Last, we observed that induction of LTD and LTP of neocortical inputs depended on the competing influence of group I mGluR and NMDA receptors, respectively. Below, we consider the significance of these observations for recognition and associative memory functions of the perirhinal cortex.

Relation between Activity-Dependent Plasticity In Vitro and Perirhinal Unit Activity in Memory Tasks

As in other cortical regions, the perirhinal cortex was previously found to express activity-dependent LTP or LTD depending on the stimulus parameters used during induction. For instance, it was first reported that repetitive bursts of high-frequency (100 Hz) afferent stimulation could produce an associative NMDA-dependent potentiation of evoked responses in perirhinal slices kept in vitro (Bilkey 1996; Ziakopoulos et al. 1999). This was not an artifact of the slice preparation as LTP of hippocampal-evoked responses could also be induced in vivo following theta-burst stimulation in field CA1 (Cousens and Otto 1998). Moreover, it was shown that low-frequency stimulation (200–900 stimuli at 1 Hz) could produce a Ca^{2+}-dependent LTD or LTP of evoked responses depending on the holding potential during induction (LTD at –70 mV; LTP at –10 mV) (Cho et al. 2001).

Subsequent studies focused on LTD because of its suspected involvement in the familiarity-induced response depressions seen in studies of recognition memory. Indeed, single-unit recording studies in rats and monkeys have shown that a proportion of perirhinal neurons display reduced responses to visual stimuli that have been presented previously, whether the animals were required to use the information to guide their behavior or not (Brown et al. 1987; Fahy et al. 1993; Li et al. 1993; Miller et al. 1993; Sobotka and Ringo 1993). These response decrements develop with a single-trial training, persist for a long time (>24 h), are manifest within 90 ms of the stimulus presentation and are more frequently encountered in the perirhinal cortex (about 25% of cells) than in the hippocampus (1%) (Riches et al. 1991; Rolls et al. 1993; Eichenbaum et al. 1996; Xiang and Brown 1998).

Correlative support for the idea that the study of activity-dependent synaptic plasticity in vitro has direct relevance for the mechanisms underlying perirhinal contributions to memory came from a series of reports where a close parallel was found between the effects of various drugs on recognition memory and LTD induction in vitro (Warburton et al. 2003;

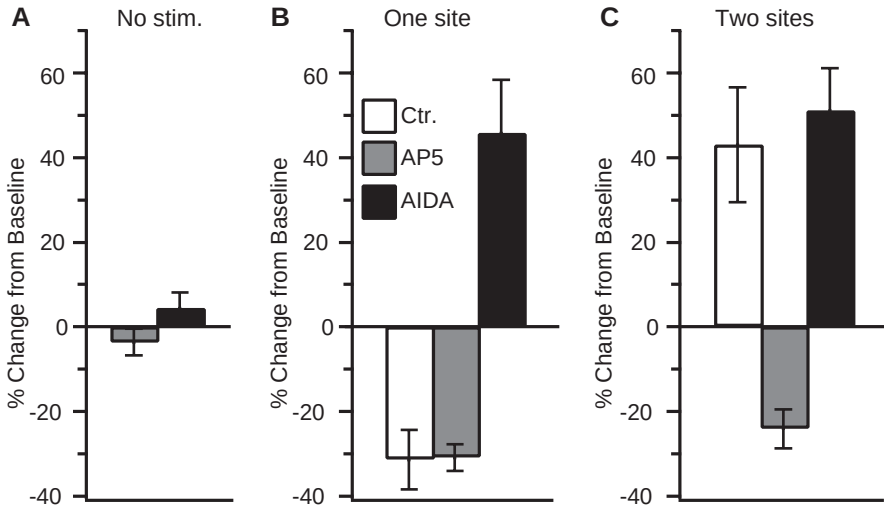

Figure 9. Induction mechanisms of LTD and LTP. Percent change in field potential response amplitude (*y*-axis; normalized to baseline) with no TFS (*A*), with TFS applied at one neocortical site (*B*), or at 2 neocortical sites simultaneously (*C*). White, gray, and black bars indicate data obtained with control perfusate, AP5, or AIDA, respectively.

Wan et al. 2004; Seoane et al. 2009). For instance, administration of the muscarinic antagonist scopolamine impaired recognition memory, reduced the familiarity-induced suppression of perirhinal firing, and blocked the induction of LTD in perirhinal slices (Warburton et al. 2003). Similarly, administration of benzodiazepines impaired both recognition memory and LTD (Wan et al. 2004).

However, other single-unit studies emphasized a different behavior of perirhinal neurons (Messinger et al. 2001; Naya, Yoshida, and Miyashita 2003) when monkeys were trained to form associations between 2 arbitrary visual stimuli. In this experimental paradigm, many neurons in area 36 and the adjacent temporal neocortex (area TE) responded selectively to some of the stimuli. However, as a result of training, many of the same neurons also became preferentially activated by the paired associate stimulus. The proportion of such pair-coding neurons was much higher in area 36 (33%) than in the adjacent temporal neocortex (5%) (Naya, Yoshida, and Miyashita 2003).

On the surface, the familiarity-induced response depressions and the emergence of pair-coding behavior in perirhinal neurons may seem contradictory. However, as argued below, the 2 phenomena can coexist and emerge from the network properties of the perirhinal cortex.

Mechanisms Underlying the Effects of TFS Depending on the Spatial Distribution of Activated Inputs

A possible explanation for the contrasting effects of TFS delivered at 1 versus 2 distant neocortical sites comes from earlier in vitro studies that examined the propagation of neocortical activity in the perirhinal cortex (Biella et al. 2001, 2002; Martina et al. 2001). Indeed, in horizontal slices of the perirhinal cortex as well as in the whole brain kept in vitro, it was found that neocortical stimuli elicit synaptic responses that propagate through the full rostrocaudal extent of the perirhinal cortex (Biella et al. 2001, 2010; Martina et al. 2001). Importantly, interruption of intrinsic neocortical versus perirhinal pathways with restricted knife cuts revealed that the propagation of neocortical activity did not occur in the neocortex but depended on longitudinal axonal pathways coursing in the perirhinal cortex itself (Martina et al. 2001), a conclusion that was corroborated in the present experiments. Moreover, these studies revealed that the responses of principal perirhinal cells to neocortical inputs was a function of whether they were in transverse register with the activated neocortical site or not: responses to adjacent sites were comprised of excitatory and inhibitory components, whereas distant ones ($\geq$1 mm) lacked the inhibitory component (Biella et al. 2001; Martina et al. 2001). In keeping with this, presumed inhibitory interneurons could only be excited by neocortical stimuli delivered in close rostrocaudal proximity whereas principal cells generated EPSPs in response to electrical stimuli delivered at rostrocaudally distant neocortical sites (Martina et al. 2001).

Overall, these results suggest that the longitudinal perirhinal pathways conveying long-range neocortical influences contact principal cells but not inhibitory interneurons (Biella et al. 2001; Martina et al. 2001). As mentioned in the introduction, both perirhinal and neocortical neurons with longitudinal axons in the perirhinal cortex support the horizontal spread of neocortical influences (Deacon et al. 1983; Room and Groenewegen 1986; Witter et al. 1986; Burwell and Amaral 1998b; Lavenex et al. 2004). In fact, the presence of a prominent system of rostrocaudally oriented intrinsic connections within the perirhinal cortex is a general property that characterizes rats (Deacon et al. 1983; Burwell and Amaral 1998b), cats (Witter et al. 1986), and monkeys (Lavenex et al. 2004), suggesting that our findings might apply to other species.

These observations have important consequences for the interpretation of the present study. Indeed, because the short- and long-range pathways conveying neocortical inputs are differentially connected to inhibitory interneurons, principal perirhinal neurons will respond distinctly depending on the spatial distribution of activated neocortical inputs. For simplicity, we first consider how the spatial distribution of neocortical inputs affects perirhinal cells in transverse register with the stimulation site. In these cells, neocortical inputs recruit perirhinal inhibitory interneurons, thus limiting the depolarization of principal cells by neocortical afferents (Fig. 10*A*, Close). When these inputs are paired with the activation of a rostrocaudally distant group of neocortical neurons (Fig.

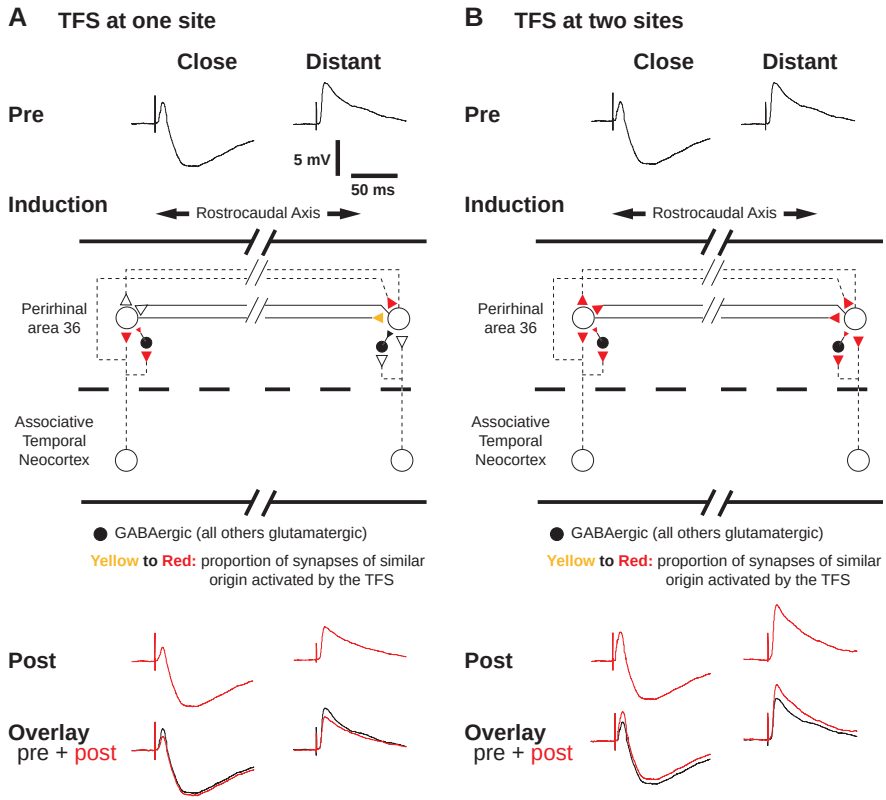

Figure 10. Hypothesized mechanisms of activity-dependent LTD and LTP induced by TFS applied at 1 (*A*) or 2 neocortical sites (*B*). Simulated synaptic responses (recorded intracellularly) elicited by neocortical stimuli are shown (Pre, Post, Overlay). In control conditions, single neocortical stimuli elicit contrasting responses at perirhinal sites in rostrocaudal proximity to (Close) versus distant (Distant) from the neocortical stimulation site. At "close sites," the neocortical elicited EPSPs are curtailed by strong feed-forward inhibition, severely limiting orthodromic firing of recipient perirhinal cells. At "distant sites," there is little recruitment of feed-forward inhibition by neocortical inputs due to the differential relationship between short- versus long-range pathways with local-circuit cells of the perirhinal cortex. (*A*) TFS is applied at one neocortical site. At close perirhinal sites, the strong recruitment of feed-forward inhibition prevents the evoked depolarization from reaching the threshold for NMDA-dependent LTP. At distant perirhinal sites, although there is less feed-forward inhibition, relatively few longitudinal glutamatergic synapses are activated. As a result, the threshold for NMDA-dependent LTP is not exceeded. Yet, at both close and distant sites, group I mGluRs are activated, leading to depression of evoked responses. (*B*) TFS is applied at 2 neocortical sites simultaneously. The convergence of inputs arising from the neocortex and longitudinal perirhinal pathways overwhelms the influence of local feed-forward inhibition. As a result, the evoked depolarization exceeds the threshold for NMDA-dependent LTP. Although group I mGluRs are activated, their depressing influence is overcome.

10*B*), this presumably shifts the balance toward excitation because long-range longitudinal pathways do not engage inhibitory interneurons. By removing the Mg^{2+} block of NMDA receptors, this increased depolarization would lead to the induction of NMDA-dependent LTP (Fig. 10*B*).

Since the long-range pathways conveying distant neocortical inputs do not contact inhibitory interneurons, why is it that TFS at a single site does not lead to LTP at rostrocaudally distant perirhinal levels? The answer likely resides in the contrasting number of synapses activated by neocortical stimuli at perirhinal levels in transverse register versus far from the stimulation site. Indeed, in baseline conditions, perirhinal response amplitudes were markedly lower (by around 60%) at a distance compared with close to the neocortical stimulation site. This suggests that much fewer synapses are involved in the long-range propagation of neocortical signals than recruited at perirhinal levels in transverse register with the neocortical stimulation site. Presumably, at distant perirhinal levels, the number of activated synapses is insufficient to bring about the critical level of depolarization required for the induction of NMDA-dependent LTP. See Figure 10 for an overview of the mechanisms hypothesized to underlie the contrasting effects of TFS applied at 1 versus 2 neocortical stimulation sites.

Yet, the fact that blocking NMDA receptors transformed the response potentiation produced by paired activation of 2 neocortical stimulation sites into a response depression suggests that synaptic efficacy in the perirhinal cortex is subjected to at least 2 competing mechanisms of regulation. In the absence of NMDA receptor activation, repetitive activation of neocortical inputs, irrespective of how much depolarization it produces, leads to a depression of synaptic efficacy. Consistent with previous in vitro experiments implicating mGluRs in perirhinal LTD (Cho et al. 2000; Jo et al. 2008), our results suggest that group I mGluR activation is critically involved in this effect. The second mechanism of regulation is NMDA receptor activation. However, in contrast with the former, this regulatory mechanism is critically dependent on the amount of depolarization produced by the stimulation conditions (Cho et al. 2001).

Returning to the apparent contradiction between familiarity-related response depressions and pair-coding behavior, the above considerations illustrate how the perirhinal network might allow both phenomena to develop, depending on the extent to which the stimulation conditions recruit the system of longitudinal perirhinal connections (Witter et al. 1986). Repeated activation of one set of neocortical inputs, as is expected to occur when a single visual stimulus is presented,

should cause a reduction of evoked responses because such stimuli would strongly excite local inhibitory interneurons with limited involvement of longitudinal connections. In contrast, activation of distributed neocortical inputs, as when different sensory stimuli have to be associated, would recruit longitudinal perirhinal connections to a higher extent and ultimately lead to a potentiation of responses evoked by the 2 paired stimuli. Moreover, since the intrinsic pathways linking different transverse perirhinal levels are reciprocal (Witter et al. 1986), subsequent activation of 1 of the 2 sets of neocortical inputs might be sufficient to reactivate the entire distributed pattern.

However, a problem with this model is that pair-coding behavior was observed even when the stimuli to be associated were presented with a delay of 1–2 s between them (for instance, see Naya, Yoshida, and Miyashita 2003). This is in contradiction with our observation that paired TFS did not cause LTP when the 2 inputs were delayed by as little as 65 ms. A possible solution to this timing problem comes from earlier single-unit studies where it was observed that perirhinal neurons display delay activity in such tasks (for instance, see Colombo and Gross 1994; Sobotka 2000; Naya, Yoshida, Takeda, et al. 2003) and from pharmacobehavioral studies implicating muscarinic-dependent persistent perirhinal activity in associating temporally distributed events (Bang and Brown 2009b). Thus, we propose that the delay activity of perirhinal neurons could bridge the temporal gap between the 2 inputs and allow for associative plasticity to take place. An important challenge for future studies will be to test these predictions in vivo.

Funding

National Institutes of Health (MH073610).

Notes

Conflict of Interest : None declared.

References

Aggleton JP, Hunt PR, Rawlins JN. 1986. The effects of hippocampal lesions upon spatial and non-spatial tests of working memory. Behav Brain Res. 19:133–146.

Bang SJ, Brown TH. 2009a. Perirhinal cortex supports acquired fear of auditory objects. Neurobiol Learn Mem. 92:52–62.

Bang SJ, Brown TH. 2009b. Muscarinic receptors in perirhinal cortex control trace conditioning. J Neurosci. 29:4346–4350.

Biella G, Gnatkovsky V, Takashima I, Kajiwara R, Iijima T, de Curtis M. 2003. Olfactory input to the parahippocampal region of the isolated guinea pig brain reveals weak entorhinal-to-perirhinal interactions. Eur J Neurosci. 18:95–101.

Biella G, Spaiardi P, Toselli M, de Curtis M, Gnatkovsky V. 2010. Functional interactions within the parahippocampal region revealed by voltage-sensitive dye imaging in the isolated guinea pig brain. J Neurophysiol. 103:725–732.

Biella G, Uva L, de Curtis M. 2001. Network activity evoked by neocortical stimulation in area 36 of the guinea pig perirhinal cortex. J Neurophysiol. 86:164–172.

Biella G, Uva L, De Curtis M. 2002. Propagation of neuronal activity along the neocortical-perirhinal-entorhinal interactions. J Neurosci. 22:9972–9979.

Bilkey DK. 1996. Long-term potentiation in the in vitro perirhinal cortex displays associative properties. Brain Res. 733:297–300.

Broadbent NJ, Squire LR, Clark RE. 2006. Reversible hippocampal lesions disrupt water maze performance during both recent and remote memory tests. Learn Mem. 13:187–191.

Brown MW, Wilson FAW, Riches IP. 1987. Neuronal evidence that inferomedial temporal cortex is more important than hippocampus in certain processes underlying recognition memory. Brain Res. 409:158–167.

Buckley MJ, Gaffan D. 1998. Learning and transfer of object-reward associations and the role of the perirhinal cortex. Behav Neurosci. 112:15–23.

Bunsey M, Eichenbaum H. 1993. Critical role of the parahippocampal region for paired-associate learning in rats. Behav Neurosci. 107:740–747.

Burwell RD, Amaral DG. 1998a. Cortical afferents of the perirhinal, postrhinal, and entorhinal cortices of the rat. J Comp Neurol. 398:179–205.

Burwell RD, Amaral DG. 1998b. Perirhinal and postrhinal cortices of the rat: interconnectivity and connections with the entorhinal cortex. J Comp Neurol. 391:293–321.

Cho K, Aggleton JP, Brown MW, Bashir ZI. 2001. An experimental test of the role of postsynaptic calcium levels in determining synaptic strength using perirhinal cortex of rat. J Physiol (London). 532:459–466.

Cho K, Kemp N, Noel J, Aggleton JP, Brown MW, Bashir ZI. 2000. A new form of long-term depression in the perirhinal cortex. Nat Neurosci. 3:150–156.

Colombo M, Gross CG. 1994. Responses of inferior temporal cortex and hippocampal neurons during delayed matching to sample in monkeys (Macaca fascicularis). Behav Neurosci. 108:443–455.

Cousens G, Otto TA. 1998. Induction and transient suppression of long-term potentiation in the peri- and postrhinal cortices following theta-related stimulation of hippocampal field CA1. Brain Res. 780:95–101.

Deacon TW, Eichenbaum H, Rosenberg P, Eckmann KW. 1983. Afferent connections of the perirhinal cortex in the rat. J Comp Neurol. 220:168–190.

de Curtis M, Pare D. 2004. The rhinal cortices: a wall of inhibition between the neocortex and hippocampus. Prog Neurobiol. 74:101–110.

de Curtis M, Pare D, Llinas RR. 1991. The electrophysiology of the olfactory-hippocampal circuit in the isolated and perfused adult mammalian brain in vitro. Hippocampus. 1:341–354.

Eacott MJ, Gaffan D, Murray EA. 1994. Preserved recognition memory for small sets, and impaired stimulus identification for large sets, following rhinal cortex ablations in monkeys. Eur J Neurosci. 6:1466–1478.

Eichenbaum H, Schoenbaum G, Young B, Bunsey M. 1996. Functional organization of the hippocampal memory system. Proc Natl Acad Sci U S A. 93:13500–13507.

Fahy FL, Riches IP, Brown MW. 1993. Neuronal activity related to visual recognition memory: long-term memory and the encoding of recency and familiarity information in the primate anterior and medial inferior temporal cortex and rhinal cortex. Exp Brain Res. 96:457–472.

Fujita S, Adachi K, Koshikawa N, Kobayashi M. 2010. Spatiotemporal dynamics of excitation in rat insular cortex: intrinsic corticocortical circuit regulates caudal-rostro excitatory propagation from the insular to frontal cortex. Neuroscience. 165:278–292.

Gaffan D, Murray EA. 1992. Monkeys (Macaca fascicularis) with rhinal cortex ablations succeed in object discrimination learning despite 24-hr intertrial intervals and fail at matching to sample despite double sample presentations. Behav Neurosci. 106:30–38.

Gnatkovsky V, de Curtis M. 2006. Hippocampus-mediated activation of superficial and deep layer neurons in the medial entorhinal cortex of the isolated guinea pig brain. J Neurosci. 26:873–881.

Gnatkovsky V, Uva L, de Curtis M. 2004. Topographic distribution of direct and hippocampus-mediated entorhinal cortex activity evoked by olfactory tract stimulation. Eur J Neurosci. 20:1897–1905.

Gonzalez-Burgos G, Barrionuevo G, Lewis DA. 2000. Horizontal synaptic connections in monkey prefrontal cortex: an in vitro electrophysiological study. Cereb Cortex. 10:82–92.

Goulet S, Murray EA. 2001. Neural substrates of crossmodal association memory in monkeys: the amygdala versus the anterior rhinal cortex. Behav Neurosci. 115:271–284.

Herzog C, Otto T. 1997. Odor-guided fear conditioning in rats: 2. Lesions of the anterior perirhinal cortex disrupt fear conditioned to the explicit conditioned stimulus but not to the training context. Behav Neurosci. 111:1265–1272.

Higuchi S, Miyashita Y. 1996. Formation of mnemonic neuronal responses to visual paired associates in inferotemporal cortex is impaired by perirhinal and entorhinal lesions. Proc Natl Acad Sci U S A. 93:739–743.

Jo J, Heon S, Kim MJ, Son GH, Park Y, Henley JM, Weiss JL, Sheng M, Collingridge GL, Cho K. 2008. Metabotropic glutamate receptor-mediated LTD involves two interacting Ca(2+) sensors, NCS-1 and PICK1. Neuron. 60:1095–1111.

Kholodar-Smith DB, Allen TA, Brown TH. 2008. Fear conditioning to discontinuous auditory cues requires perirhinal cortical function. Behav Neurosci. 122:1178–1185.

Lavenex P, Suzuki WA, Amaral DG. 2004. Perirhinal and parahippocampal cortices of the macaque monkey: intrinsic projections and interconnections. J Comp Neurol. 472:371–394.

Leonard BW, Amaral DG, Squire LR, Zola-Morgan S. 1995. Transient memory impairment in monkeys with bilateral lesions of the entorhinal cortex. J Neurosci. 15:5367–5659.

Li L, Miller EK, Desimone R. 1993. The representation of stimulus familiarity in anterior inferior temporal cortex. J Neurophysiol. 69:1918–1929.

Lindquist DH, Jarrard LE, Brown TH. 2004. Perirhinal cortex supports delay fear conditioning to rat ultrasonic social signals. J Neurosci. 24:3610–3617.

Martina M, Royer S, Paré D. 2001. Propagation of neocortical inputs in the perirhinal cortex. J Neurosci. 21:2878–2888.

Melchitzky DS, Sesack SR, Pucak ML, Lewis DA. 1998. Synaptic targets of pyramidal neurons providing intrinsic horizontal connections in monkey prefrontal cortex. J Comp Neurol. 390:211–224.

Messinger A, Squire LR, Zola SM, Albright TD. 2001. Neuronal representations of stimulus associations develop in the temporal lobe during learning. Proc Natl Acad Sci U S A. 98:12239–12244.

Meunier M, Bachevalier J, Mishkin M, Murray EA. 1993. Effects on visual recognition of combined and separate ablations of the entorhinal and perirhinal cortex in rhesus monkeys. J Neurosci. 13:5418–5432.

Meunier M, Hadfield W, Bachevalier J, Murray EA. 1996. Effects of rhinal cortex lesions combined with hippocampectomy on visual recognition memory in rhesus monkeys. J Neurophysiol. 75:1190–1205.

Miller EK, Li L, Desimone R. 1993. Activity of neurons in anterior inferior temporal cortex during a short-term memory task. J Neurosci. 13:1460–1478.

Muhlethaler M, de Curtis M, Walton K, Llinas R. 1993. The isolated and perfused brain of the guinea-pig in vitro. Eur J Neurosci. 5:915–926.

Mumby DG, Pinel J. 1994. Rhinal cortex lesions and object recognition in rats. Behav Neurosci. 108:11–18.

Murray EA, Gaffan EA, Mishkin M. 1993. Neural substrate of visual stimulus-stimulus association in rhesus monkey. J Neurosci. 13:4549–4561.

Murray EA, Graham KS, Gaffan D. 2005. Perirhinal cortex and its neighbours in the medial temporal lobe: contributions to memory and perception. Q J Exp Psychol B. 58:378–396.

Murray EA, Mishkin M. 1986. Visual recognition in monkeys following rhinal cortical ablations combined with either amygdalectomy or hippocampectomy. J Neurosci. 6:1991–2003.

Naya Y, Yoshida M, Miyashita Y. 2003. Forward processing of long-term associative memory in monkey. J Neurosci. 23:2861–2871.

Naya Y, Yoshida M, Takeda M, Fujimichi R, Miyashita Y. 2003. Delay-period activities in two subdivisions of monkey inferotemporal cortex during pair association memory task. Eur J Neurosci. 18:2915–2918.

Parker A, Gaffan D. 1998. Lesions of the primate rhinal cortex cause deficits in flavour-visual associative memory. Behav Brain Res. 93:99–105.

Pinto A, Fuentes C, Pare D. 2006. Feedforward inhibition regulates perirhinal transmission of neocortical inputs to the entorhinal cortex: ultrastructural study in guinea pigs. J Comp Neurol. 495:722–734.

Riches IP, Wilson FA, Brown MW. 1991. The effects of visual stimulation and memory on neurons of the hippocampal formation and the neighboring parahippocampal gyrus and inferior temporal cortex of the primate. J Neurosci. 11:1763–1779.

Rolls ET, Cahusac P, Feigenbaum JD, Miyashita Y. 1993. Responses of single neurons in the hippocampus of the macaque related to recognition memory. Exp Brain Res. 93:299–306.

Room P, Groenewegen HJ. 1986. Connections of the parahippocampal cortex. I. Cortical afferents. J Comp Neurol. 251:415–450.

Seoane A, Massey PV, Keen H, Bashir ZI, Brown MW. 2009. L-type voltage-dependent calcium channel antagonists impair perirhinal long-term recognition memory and plasticity processes. J Neurosci. 29:9534–9544.

Sobotka S. 2000. Involvement of single unit activity in inferotemporal and perirhinal cortices in recognition memory of visual objects in the macaque. Acta Neurobiol Exp (Wars). 60:219–226.

Sobotka S, Ringo JL. 1993. Investigation of long-term recognition and association memory in unit responses from inferotemporal cortex. Exp Brain Res. 96:28–38.

Suzuki WA. 1996. The anatomy, physiology and functions of the perirhinal cortex. Curr Opin Neurobiol. 6:179–186.

Suzuki WA, Amaral DG. 1994. Perirhinal and parahippocampal cortices of the macaque monkey: cortical afferents. J Comp Neurol. 350:497–533.

Suzuki WA, Zola-Morgan S, Squire LR, Amaral DG. 1993. Lesions of the perirhinal and parahippocampal cortices in the monkey produce long-lasting memory impairment in the visual and tactual modalities. J Neurosci. 13:2430–2451.

Tehovnik EJ, Sommer MA. 1997. Effective spread and timecourse of neural inactivation caused by lidocaine injection in monkey cerebral cortex. J Neurosci Methods. 74:17–26.

Uva L, de Curtis M. 2005. Polysynaptic olfactory pathway to the ipsi- and contralateral entorhinal cortex are mediated via the hippocampus. Neuroscience. 130:249–258.

Uva L, Gruschke S, Biella G, de Curtis M, Witter MP. 2004. Cytoarchitectonic characterization of the parahippocampal region of the guinea pig. J Comp Neurol. 474:289–303.

Wan H, Warburton EC, Zhu XO, Koder TJ, Park Y, Aggleton JP, Cho K, Bashir ZI, Brown MW. 2004. Benzodiazepine impairment of perirhinal cortical plasticity and recognition memory. Eur J Neurosci. 20:2214–2224.

Warburton EC, Koder T, Cho K, Massey PV, Duguid G, Barker GRI, Aggleton JP, Bashir ZI, Brown MW. 2003. Cholinergic neurotransmission is essential for perirhinal cortical plasticity and recognition memory. Neuron. 38:987–996.

Witter MP, Room P, Groenewegen HJ, Lohman AHM. 1986. Connections of the parahippocampal cortex in the cat. V. Intrinsic connections; comments on input/output connections with the hippocampus. J Comp Neurol. 252:78–94.

Witter MP, Wouterlood FG, Naber PA, Van Haeften T. 2000. Anatomical organization of the parahippocampal-hippocampal network. Ann N Y Acad Sci. 911:1–24.

Xiang JZ, Brown MW. 1998. Differential neuronal encoding of novelty, familiarity and recency in regions of the anterior temporal lobe. Neuropharmacology. 37:657–676.

Ziakopoulos Z, Tillett CW, Brown MW, Bashir ZI. 1999. Input- and layer-dependent synaptic plasticity in the rat perirhinal cortex in vitro. Neuroscience. 92:459–472.

Zola-Morgan S, Squire LR, Amaral DG, Suzuki WA. 1989. Lesions of perirhinal and parahippocampal cortex that spare the amygdala and hippocampal formation produce severe memory impairment. J Neurosci. 9:4355–4370.

Zola-Morgan S, Squire LR, Clower RP, Rempel NL. 1993. Damage to the perirhinal cortex exacerbates memory impairment following lesions to the hippocampal formation. J Neurosci. 13:251–265.